

PREDICTION OF MELTING PROFILE OF MILD STEEL WELD METALS USING REGRESSION ANALYSIS

Onoriode K. Idiapho^{1*}, Raphael Biu¹ and William E. Odinikuku² and Onomine M. Akusu²

¹Department of Production Engineering, University of Benin, Nigeria.

²Department of Mechanical Engineering, Petroleum Training Institute, Warri, Nigeria.

Authors' contributions

This work was carried out in collaboration between all authors. All authors read and approved the final manuscript.

ABSTRACT

The microstructure of a weldment can be maintained by ensuring a steady state homogenous melting profile of the welding operation, which includes the deposition of optimum volumes of melted filler wire and substantial part of the heat affected zones of the parent metal to form the weld pool. The melting pattern of the entire welding process should be protected from atmospheric air, so as to enhance weldment quality. In this study, the melting profile of mild steel is investigated by looking at the parent metal angular distortion bead width and penetration volumes of deposited filler and the melting efficiency was determined. Predictive models were also developed to determine the above listed melting properties by applying the regression analysis. The result obtained showed that, there is almost a perfect fit between the calculated and predicted angular distortion, as well as between the calculated and predicted volume of filler wire melted. There is also a close correlation between the calculated and predicted melting efficiency. However, for the bead width, bead penetration and volume of weld metal deposited, there were variations of values and a heterogeneous correlation between the calculated, measured and predicted values. The effects of the process parameters on the obtained properties of the melting profile were investigated and optimum process parameters were determined.

Keywords: melting profile, mild steel, melting efficiency, regression analysis,

1. INTRODUCTION

Local welders in Nigeria are prone to poor quality weldment because of their lack of technical welding skills. When these local welders carry out their welding operations, the welded joints are considered to be good enough just because the metal materials welded together are seen to be good and satisfactory. In most cases, these welded joints do not serve their useful life due to the poor quality of the weldment. Material quality can easily be assessed by inspecting the microstructure of the weldment. However, what determines the behavior and characteristics of the weld microstructure is the weldmetal melting profile. When the filler wire and the heat affected zones of the parent material melt to form the weld pool, the melting process may be in such a way that there may be significant entrance of the atmospheric air into the molten weldmetal or there may not be sufficient arc heat to produce a homogenous weldmetal flow pattern. The solidified welded joint product may contain a poor microstructure. The melting profile of the filler wire has a very significant impact on the microstructure of welded joints. It is suggested that the combination of process parameters should be well optimized to avoid the production of poor weldment. Aside from the optimization of process parameters, prediction of the resultant output parameters in relation to some combination of input parameters can further eliminate the cost of optimization process and the time spent on the optimization process. Predicted combination of process parameters give near optimal output parameters. In most cases the difference between the experimental results and the predicted results are evaluated. However, the difference is usually denoted as the error. The smaller the error between the experimental and predicted results, the more potent the predictive model or equation applied.

Researchers in the past, such as Lee and Um [1], predicted welding process parameters using multiple regression analysis and artificial neural network. The prediction results showed low error enough to be applied to real welding. Gunaraj and Murugan [2] predicted and optimized weldbead volume for submerged arc welding process using a five level, four factor, central composite rotatable factorial design consisting of thirty one sets of cooled conditions. Sreeraj et al. [3] in a gas metal arc welding process using response surface methodology and Fmincon. The developed model was checked for adequacy and the process parameters were optimized by using the Fmincon function. Lalitnarayan et al. [4] predicted the weld bead geometry for CO₂ welding process using multiple regression analysis. Karthikeyan and Balasubramanian [5] predicted the optimized friction stir spot welding process parameters for joining AA2024 aluminum. These authors used a central composite rotatable design with four factors and five levels to minimize the number of experimental conditions. An empirical relationship was established to predict the tensile shear fracture load of friction stir spot welded AA2024 aluminum alloy by incorporating independently controllable Friction Stir Spot Welding (FSSW) process parameters. Response surface methodology was applied to optimize the FSSW parameters to attain maximum lap shear strength of spot weld. In this study, the weld metal melting profile of Gas Metal Arc Welding (GMAW) mild steel weld is investigated using the regression method.

2. MATERIALS AND METHODS

2.1 MATERIALS

The Gas Metal Arc Welding (GMAW) was used to weld 4 mm mild steel. The input parameters used for this study are current, voltage, welding speed and welding angle. The welding machines contain the welding gun, shielding gas consisting of 80% argon and 20% carbon dioxide. A 3.2 mm consumable wire electrode of AWS classification ER70S-3 was used for the welding operation. The Brinell hardness tester was used in this study to determine the weld or test specimen's hardness number. The higher the Brinell hardness number (BHN), the harder the specimen becomes. The sixteen process parameters were used to make weldments. Each combination of process parameters were used to make five weldments and each of these weldments were bisected. The bead heights of each of the five weldments were measured using a caliper micrometer and the average value of the bead heights was recorded. Eighty weldments were made with the sixteen process parameters and sixteen average values of the bead heights were recorded. Power saw was used to cut the weld bead so that the bead height can be measured. It functions by drawing a blade containing teeth through the work piece. The sawing machine is preferred to the hand saw because it is faster and easier and principally produces an accurate square or mitered cut on the workpiece. The power hacksaw is used for squared or angle cutting of metal. It uses a reciprocating (back and forth) cutting action.

2.2 METHODS

The following equations were used to determine the output process parameters Artem Pilipenko [6] reported a relationship for Angular distortion, α .

$$\alpha = 0.13 \frac{IV}{St^2} \quad (1)$$

Where I = current in amperes

V = voltage

S = welding speed, m/s

t = plate thickness in metres

Volume of weldmetal deposited per second (mm^2/s), V_{wd}

$$V_{wd} = pbs \quad (2)$$

Where

b = weld bead width, mm

p = weld bead depth or penetration, mm

s = welding speed, mm/s

Volume of wire melted

$$V_{wire} = W_{wire} \times \pi r_w^2 \quad (3)$$

r_w = wire radius

Where W_{wire} = wire feed rate

$$\text{Filler wire area, } F_a = \frac{\pi d_{el}^2}{4} \text{ Ivanov and Ulanov [7]} \quad (4)$$

d_{el} = diameter of electrode wire

$$\text{Melting efficiency, } \eta_m = \frac{E_{im} V_{im} + E_s V_s}{\eta_a V I t} \text{ Dupont and Marder [8]} \quad (5)$$

Where E_{im} = Energy required to raise the filler metal to the melting point = $0.165 \times 10^4 L/mm^3 = 65s^{-1}$

E_s = Energy required to raise the substrate to the melting point = $0.95 \times 10^4 L/mm^3 = 95s^{-1}$

V_{im} = Volume of deposited filler metal

V_s = Volume of metal deposited per second

η_a = Arc efficiency, for GMAW = 0.80 Dupont and Marder [8]

V = Voltage

I = Current

t = Welding time, seconds.

3. RESULTS AND DISCUSSION

3.1 RESULTS

Table 1 shows the input and output process parameters which comprise of eighteen (18) welding runs. Each input parameter was used to make weldments and the corresponding output parameters contain the average values obtained for them.

From Table 1, using the melting efficiency as an optimization criterion, the welding process parameters of welding experiment one (1), would be the optimized process parameters.

Table 1. Input and Output process parameters

Exp No	INPUTS					OUTPUTS					
	Welding Speed (mm/s)	Current (A)	Wire feed rate (mm/s)	Voltage (V)	Time (sec)	Angular distortion, α (°)	Bead width (mm)	Bead penetration (mm)	Vol weld metal deposited per second (mm ³ /s)	Volume of wire melted (mm ³ /s)	Melting efficiency (%)
1	2.42	210	41.67	24	12	2.71	8.50	9.24	190.07	83.76	49
2	2.42	290	58.33	29	18	4.52	8.10	5.14	100.75	117.24	14
3	2.42	350	91.67	36	23	6.77	12.20	7.18	210.51	184.26	14
4	2.67	210	41.67	29	18	2.97	12.80	10.12	345.86	83.76	44
5	2.67	290	58.33	36	23	5.08	5.20	8.25	114.54	117.24	10
6	2.67	350	91.67	24	12	4.09	9.75	4.39	114.28	184.26	28
7	2.83	210	58.33	24	23	2.32	6.10	11.26	194.38	117.24	28
8	2.83	290	91.67	29	12	3.86	5.85	10.76	178.14	184.26	36
9	2.83	350	41.67	36	18	5.79	10.25	11.00	319.08	83.76	20
10	2.42	210	91.67	36	18	4.06	8.92	5.63	121.53	184.26	22
11	2.42	290	41.67	24	23	3.74	7.15	4.66	80.63	83.76	10
12	2.42	350	58.33	29	12	5.45	7.05	9.81	167.37	117.24	24
13	2.67	210	58.33	36	12	3.68	8.16	6.42	139.87	117.24	29
14	2.67	290	91.67	24	18	3.39	3.25	8.42	73.06	184.26	19
15	2.67	350	41.67	29	23	4.94	8.22	6.96	152.75	83.76	11
16	2.83	210	91.67	29	23	2.80	3.03	4.94	42.36	184.26	14
17	2.83	290	41.67	36	12	4.80	12.47	9.22	325.38	83.76	36
18	2.83	350	58.33	24	18	3.86	10.82	6.31	193.22	117.76	22

Linear Regression Model

Utilizing the linear regression analysis method, the angular distortion of the mild steel plate is considered here.

1. Angular distortion, α

Table 2 contains the goodness fit coefficients of the linear regression analysis conducted.

Table 2. Goodness of fit coefficients for angular distortion

R (coefficient of correlation)	0.991
R ² (coefficient of determination)	0.982
R ² adj. (adjusted coefficient of determination)	0.974
SSR	0.418

Table 3 contains the statistical model parameters determined for the angular distortion.

Table 3. Model Parameters for Angular Distortion

Parameter	Value	Standard deviation	Student's t	Pr > t	Lower bound 95 %	Upper bound 95 %
Intercept	-0.206	0.801	-0.257	0.802	-1.951	1.540
Welding Speed (mm/s)	-1.598	0.261	-6.126	< 0.0001	-2.166	-1.030
Current (A)	0.015	0.001	19.143	< 0.0001	0.013	0.016
Wire feed rate (mm/s)	0.000	0.002	0.047	0.963	-0.005	0.005
Voltage (V)	0.140	0.009	15.601	< 0.0001	0.120	0.159
Time (sec)	0.016	0.010	1.587	0.138	-0.006	0.037

From Table 3, the Predictive model obtained is expressed in Eq. (6)

$$\text{Model equation: } \alpha = -0.206 - 1.598*S + 0.015*I + 0.140*V + 0.016t \quad (6)$$

The predictive model in Eq. (6) is used to determine the predicted angular distortion values that compare with the calculated values in Table 4.

Table 4. Predicted Angular Distortion

Exp Number	Weights	Angular distortion, $\alpha(^{\circ})$	Angular distortion, $\alpha(^{\circ})$ (Predicted)	Residuals	Standardized residuals	Lower Conf. Mean	Upper Conf. Mean	Lower Conf. Individ.	Upper Conf. Individ.
1	1	2.710	2.551	0.159	0.853	2.273	2.829	2.058	3.043
2	1	4.520	4.518	0.002	0.009	4.358	4.679	4.081	4.956
3	1	6.770	6.457	0.313	1.675	6.171	6.743	5.960	6.955
4	1	2.970	2.942	0.028	0.150	2.754	3.130	2.494	3.390
5	1	5.080	5.173	-0.093	-0.498	4.977	5.369	4.721	5.625
6	1	4.090	4.213	-0.123	-0.658	3.958	4.468	3.733	4.693
7	1	2.320	2.068	0.252	1.349	1.820	2.316	1.591	2.545
8	1	3.860	3.773	0.087	0.464	3.545	4.002	3.307	4.240
9	1	5.790	5.719	0.071	0.378	5.476	5.962	5.246	6.193
10	1	4.060	4.323	-0.263	-1.408	4.055	4.590	3.836	4.810
11	1	3.740	3.897	-0.157	-0.840	3.651	4.143	3.421	4.372
12	1	5.450	5.307	0.143	0.768	5.077	5.536	4.839	5.774
13	1	3.680	3.827	-0.147	-0.787	3.592	4.061	3.357	4.297
14	1	3.390	3.425	-0.035	-0.186	3.229	3.620	2.973	3.876
15	1	4.940	5.076	-0.136	-0.730	4.863	5.290	4.617	5.536
16	1	2.800	2.769	0.031	0.166	2.513	3.025	2.288	3.249
17	1	4.800	4.745	0.055	0.295	4.497	4.992	4.269	5.221
18	1	3.860	4.047	-0.187	-1.002	3.832	4.262	3.587	4.507

2. Bead width

Table 5 contains the goodness fit coefficients of the linear regression analysis conducted for bead width.

Table 5. Goodness of fit coefficients for bead width

R (coefficient of correlation)	0.577
R ² (coefficient of determination)	0.333
R ² adj. (adjusted coefficient of determination)	0.056
SSR	94.714

Table 6 contains the statistical model parameters determined for the bead width.

Table 6. Model parameters for bead width

Parameter	Value	Standard deviation	Student's t	Pr > t	Lower bound 95 %	Upper bound 95 %
Intercept	9.564	12.056	0.793	0.443	-16.703	35.831
Welding Speed (mm/s)	-1.527	3.925	-0.389	0.704	-10.078	7.025
Current (A)	0.012	0.012	0.998	0.338	-0.014	0.037
Wire feed rate (mm/s)	-0.049	0.032	-1.524	0.153	-0.118	0.021
Voltage (V)	0.170	0.135	1.262	0.231	-0.123	0.463
Time (sec)	-0.143	0.147	-0.968	0.352	-0.463	0.178

From Table 6, the Predictive model obtained is expressed in Eq. (7)

$$\text{Model equation: } w = 9.564 - 1.527*S + 0.012*I - 0.049*f + 0.170*V - 0.143*t \quad (7)$$

The predictive model in Eq. (7) is used to determine the predicted bead width values that compare with the calculated values in Table 7.

Table 7. Predicted Bead Widths

Exp Number	Weights	Bead width (mm)	Bead width (mm) (Predicted)	Residuals	Standardized residuals	Lower Conf. Mean	Upper Conf. Mean	Lower Conf. Individ.	Upper Conf. Individ.
1	1	8.500	8.628	-0.128	-0.046	4.449	12.808	1.216	16.040
2	1	8.100	8.734	-0.634	-0.226	6.316	11.152	2.153	15.316
3	1	12.200	8.282	3.918	1.395	3.977	12.586	0.799	15.765
4	1	12.800	8.240	4.560	1.623	5.415	11.065	1.498	14.981
5	1	5.200	8.828	-3.628	-1.291	5.878	11.777	2.033	15.622
6	1	9.750	7.432	2.318	0.825	3.592	11.271	0.206	14.658
7	1	6.100	5.625	0.475	0.169	1.888	9.361	-1.547	12.796
8	1	5.850	7.345	-1.495	-0.532	3.908	10.782	0.325	14.365
9	1	10.250	10.797	-0.547	-0.195	7.140	14.453	3.666	17.927
10	1	8.920	7.382	1.538	0.548	3.357	11.407	0.056	14.708
11	1	7.150	7.981	-0.831	-0.296	4.278	11.685	0.827	15.136
12	1	7.050	10.281	-3.231	-1.150	6.828	13.735	3.253	17.309
13	1	8.160	9.475	-1.315	-0.468	5.946	13.003	2.409	16.540
14	1	3.250	5.885	-2.635	-0.938	2.941	8.828	-0.907	12.677
15	1	8.220	9.140	-0.920	-0.327	5.930	12.350	2.228	16.052
16	1	3.030	4.855	-1.825	-0.649	1.006	8.703	-2.376	12.085
17	1	12.470	10.961	1.509	0.537	7.235	14.687	3.795	18.127
18	1	10.820	7.951	2.869	1.021	4.718	11.184	1.028	14.874

3. Bead penetration, p

Table 8 contains the goodness fit coefficients of the linear regression analysis conducted for bead penetration.

Table 8. Goodness of fit coefficient for bead penetration

R (coefficient of correlation)	0.507
R ² (coefficient of determination)	0.257
R ² adj. (adjusted coefficient of determination)	-0.052
SSR	68.112

Table 9 contains the statistical model parameters determined for the bead penetration.

Table 9. Model parameters for bead penetration

Parameter	Value	Standard deviation	Student's t	Pr > t	Lower bound 95 %	Upper bound 95 %
Intercept	-1.093	10.223	-0.107	0.917	-23.368	21.182
Welding Speed (mm/s)	4.556	3.328	1.369	0.196	-2.695	11.808
Current (A)	-0.002	0.010	-0.239	0.815	-0.024	0.019
Wire feed rate (mm/s)	-0.032	0.027	-1.200	0.253	-0.091	0.026
Voltage (V)	0.044	0.114	0.389	0.704	-0.204	0.293
Time (sec)	-0.100	0.125	-0.797	0.441	-0.372	0.173

From Table 9, the Predictive model obtained is expressed in Eq. (8)

$$\text{Model equation: } p = - 1.093 + 4.556*S - 0.002*I - 0.032*f + 0.044*V - 0.100*t \quad (8)$$

The predictive model in Eq. (8) is used to determine the predicted bead penetration values that compare with the calculated values in Table 10.

Table 10. Predicted Bead Penetrations

Exp Number	Weights	Bead penetration (mm)	Bead penetration (mm) (Predicted)	Residuals	Standardized residuals	Lower Conf. Mean	Upper Conf. Mean	Lower Conf. Individ.	Upper Conf. Individ.
1	1	9.240	7.963	1.277	0.536	4.419	11.508	1.678	14.249
2	1	5.140	6.861	-1.721	-0.722	4.811	8.912	1.280	12.442
3	1	7.180	5.453	1.727	0.725	1.803	9.103	-0.892	11.799
4	1	10.120	8.727	1.393	0.585	6.332	11.123	3.010	14.444
5	1	8.250	7.814	0.436	0.183	5.312	10.315	2.051	13.576
6	1	4.390	7.154	-2.764	-1.160	3.898	10.410	1.027	13.282
7	1	11.260	8.197	3.063	1.286	5.028	11.365	2.115	14.278
8	1	10.760	8.245	2.515	1.055	5.331	11.160	2.292	14.198
9	1	11.000	9.440	1.560	0.655	6.339	12.541	3.393	15.487
10	1	5.630	6.278	-0.648	-0.272	2.865	9.691	0.066	12.491
11	1	4.660	6.682	-2.022	-0.849	3.541	9.822	0.615	12.749
12	1	9.810	7.318	2.492	1.046	4.389	10.247	1.358	13.278
13	1	6.420	9.095	-2.675	-1.123	6.103	12.088	3.103	15.087
14	1	8.420	6.697	1.723	0.723	4.201	9.193	0.938	12.457
15	1	6.960	7.903	-0.943	-0.396	5.180	10.625	2.041	13.764
16	1	4.940	7.338	-2.398	-1.006	4.075	10.601	1.206	13.469
17	1	9.220	10.177	-0.957	-0.402	7.018	13.337	4.100	16.254
18	1	6.310	8.367	-2.057	-0.863	5.625	11.109	2.496	14.238

4. Volume of weld metal deposited per second, V_m

Table 11 contains the goodness of fit coefficients of the linear regression analysis conducted for volume of weld metal deposited per second.

Table 11. Goodness of fit coefficients for volume of weld metal deposited per second

R (coefficient of correlation)	0.709
R ² (coefficient of determination)	0.503
R ² adj. (adjusted coefficient of determination)	0.296
SSR	63944.206

Table 12 contains the statistical model parameters determined for the volume of weld metal deposited per second.

Table 12. Model parameters for volume of weld metal deposited per second

Parameter	Value	Standard deviation	Student's t	Pr > t	Lower bound 95 %	Upper bound 95 %
Intercept	-194.961	313.248	-0.622	0.545	-877.469	487.547
Welding Speed (mm/s)	145.605	101.978	1.428	0.179	-76.585	367.795
Current (A)	0.120	0.300	0.402	0.695	-0.533	0.774
Wire feed rate (mm/s)	-2.047	0.828	-2.473	0.029	-3.850	-0.243
Voltage (V)	5.380	3.496	1.539	0.150	-2.237	12.997
Time (sec)	-4.653	3.826	-1.216	0.247	-12.989	3.684

From Table 12, the Predictive model obtained is expressed in Eq. (9)

The predictive model in Eq. (9) is used to determine the predicted volume of weld metal deposited per second values that compare with the calculated values in Table 13.

$$\text{Model equation: } V_m = -194.961 + 145.605 \cdot S + 0.120 \cdot I - 2.047 \cdot f + 5.380 \cdot V - 4.653 \cdot t \quad (9)$$

Table 13. Predicted volume of weld metal deposited per second

Exp Number	Weights	Vol weld metal deposited per second (mm ³ /s)	Vol weld metal deposited per second (mm ³ /s) (Predicted)	Residuals	Standardized residuals	Lower Conf. Mean	Upper Conf. Mean	Lower Conf. Individ.	Upper Conf. Individ.
1	1	190.070	170.700	19.370	0.265	62.104	279.296	-21.886	363.287
2	1	100.750	145.223	-44.473	-0.609	82.391	208.055	-25.787	316.232
3	1	210.510	98.608	111.902	1.533	-13.230	210.446	-95.825	293.041
4	1	345.860	206.086	139.774	1.915	132.690	279.481	30.919	381.252
5	1	114.540	196.020	-81.480	-1.116	119.383	272.658	19.471	372.570
6	1	114.280	121.628	-7.348	-0.101	21.862	221.395	-66.121	309.378
7	1	194.380	145.120	49.260	0.675	48.033	242.207	-41.219	331.459
8	1	178.140	164.596	13.544	0.186	75.300	253.892	-17.805	346.998
9	1	319.080	283.909	35.171	0.482	188.896	378.921	98.642	469.175
10	1	121.530	105.004	16.526	0.226	0.421	209.587	-85.348	295.356
11	1	80.630	129.160	-48.530	-0.665	32.934	225.385	-56.732	315.052
12	1	167.370	180.367	-12.997	-0.178	90.635	270.099	-2.248	362.982
13	1	139.870	237.561	-97.691	-1.338	145.871	329.251	53.976	421.146
14	1	73.060	86.484	-13.424	-0.184	10.003	162.966	-89.998	262.966
15	1	152.750	199.689	-46.939	-0.643	116.279	283.099	20.096	379.282
16	1	42.360	103.780	-61.420	-0.841	3.790	203.769	-84.088	291.647
17	1	325.380	304.596	20.784	0.285	207.791	401.400	118.403	490.788
18	1	193.220	185.250	7.970	0.109	101.238	269.262	5.376	365.123

5. Volume of wire melted, V_w

Table 14 contains the goodness fit coefficients of the linear regression analysis conducted for volume of wire melted.

Table 14. Goodness of fit coefficients for volume of wire melted.

R (coefficient of correlation)	1.000
R ² (coefficient of determination)	1.000
R ² adj. (adjusted coefficient of determination)	1.000
SSR	0.191

Table 15 contains the statistical model parameters determined for the volume of wire melted.

Table 15. Model parameters for volume of wire melted

Parameter	Value	Standard deviation	Student's t	Pr > t	Lower bound 95 %	Upper bound 95 %
Intercept	-0.431	0.541	-0.797	0.441	-1.610	0.748
Welding Speed (mm/s)	0.193	0.176	1.095	0.295	-0.191	0.577
Current (A)	0.001	0.001	1.130	0.280	-0.001	0.002
Wire feed rate (mm/s)	2.010	0.001	1405.934	< 0.0001	2.007	2.013
Voltage (V)	-0.007	0.006	-1.119	0.285	-0.020	0.006
Time (sec)	0.000	0.007	0.072	0.944	-0.014	0.015

From Table 15, the Predictive model obtained is expressed in Eq. (10)

The predictive model in Eq. (10) is used to determine the predicted volume of wire melted values that compare with the calculated values in Table 16.

$$\text{Model equation: } V_w = -0.431 + 0.193*S + 0.001*I + 2.010*f - 0.007*V \quad (10)$$

Table 16. Predicted volume of wire melted.

Exp Numbers	Weights	Volume of wire melted (mm ³ /s)	Volume of wire melted (mm ³ /s) (Predicted)	Residuals	Standardized residuals	Lower Conf. Mean	Upper Conf. Mean	Lower Conf. Indiv.	Upper Conf. Indiv.
1	1	83.760	83.745	0.015	0.123	83.557	83.932	83.412	84.077
2	1	117.240	117.241	-0.001	-0.011	117.133	117.350	116.946	117.537
3	1	184.260	184.234	0.026	0.210	184.040	184.427	183.898	184.569
4	1	83.760	83.762	-0.002	-0.014	83.635	83.889	83.459	84.064
5	1	117.240	117.245	-0.005	-0.037	117.112	117.377	116.940	117.550
6	1	184.260	184.358	-0.098	-0.774	184.185	184.530	184.033	184.682
7	1	117.240	117.310	-0.070	-0.553	117.142	117.477	116.988	117.632
8	1	184.260	184.319	-0.059	-0.472	184.165	184.474	184.004	184.634
9	1	83.760	83.827	-0.067	-0.534	83.663	83.991	83.507	84.147
10	1	184.260	184.149	0.111	0.879	183.969	184.330	183.820	184.478
11	1	83.760	83.797	-0.037	-0.291	83.630	83.963	83.476	84.118
12	1	117.240	117.274	-0.034	-0.267	117.119	117.429	116.958	117.589
13	1	117.240	117.193	0.047	0.376	117.034	117.351	116.875	117.510
14	1	184.260	184.325	-0.065	-0.518	184.193	184.457	184.021	184.630
15	1	83.760	83.846	-0.086	-0.684	83.702	83.990	83.536	84.156
16	1	184.260	184.278	-0.018	-0.142	184.105	184.451	183.953	184.602
17	1	83.760	83.789	-0.029	-0.233	83.622	83.957	83.468	84.111
18	1	117.760	117.389	0.371	2.940	117.244	117.534	117.079	117.700

6. Melting efficiency, η

Table 17 contains the goodness fit coefficients of the linear regression analysis conducted for melting efficiency.

Table 17. Goodness of fit coefficients for melting efficiency

R (coefficient of correlation)	0.858
R ² (coefficient of determination)	0.736
R ² adj. (adjusted coefficient of determination)	0.626
SSR	602.651

Table 18 contains the statistical model parameters determined for the melting efficiency.

Table 18. Model parameters for melting efficiency

Parameter	Value	Standard deviation	Student's t	Pr > t	Lower bound 95 %	Upper bound 95 %
Intercept	70.879	30.410	2.331	0.038	4.620	137.137
Welding Speed (mm/s)	8.997	9.900	0.909	0.381	-12.573	30.567
Current (A)	-0.082	0.029	-2.826	0.015	-0.146	-0.019
Wire feed rate (mm/s)	-0.101	0.080	-1.262	0.231	-0.276	0.074
Voltage (V)	-0.343	0.339	-1.011	0.332	-1.083	0.396
Time (sec)	-1.741	0.371	-4.687	0.001	-2.550	-0.932

From Table 18, the Predictive model obtained is expressed in Eq. (11)

The predictive model in Eq. (11) is used to determine the predicted melting efficiency values that compare with the calculated values in Table 19.

$$\text{Model equation: } \eta = 70.879 + 8.997*S - 0.082*I - 0.101*f - 0.343*V - 1.741*t$$

(11)

Table 19. Predicted melting efficiency

Exp Number	Weights	Melting efficiency (%)	Melting efficiency (%) (Predicted)	Residuals	Standardized residuals	Lower Conf. Mean	Upper Conf. Mean	Lower Conf. Individ.	Upper Conf. Individ.
1	1	49.000	42.010	6.990	0.986	31.467	52.552	23.313	60.706
2	1	14.000	21.573	-7.573	-1.069	15.473	27.673	4.971	38.175
3	1	14.000	2.146	11.854	1.673	-8.711	13.003	-16.730	21.022
4	1	44.000	32.097	11.903	1.680	24.972	39.223	15.092	49.103
5	1	10.000	12.715	-2.715	-0.383	5.275	20.155	-4.424	29.855
6	1	28.000	27.664	0.336	0.047	17.978	37.349	9.437	45.890
7	1	28.000	24.860	3.140	0.443	15.434	34.285	6.770	42.950
8	1	36.000	32.326	3.674	0.518	23.657	40.995	14.618	50.034
9	1	20.000	19.609	0.391	0.055	10.385	28.833	1.623	37.595
10	1	22.000	22.375	-0.375	-0.053	12.222	32.528	3.895	40.854
11	1	10.000	16.275	-6.275	-0.885	6.933	25.616	-1.772	34.321
12	1	24.000	27.079	-3.079	-0.434	18.368	35.790	9.351	44.807
13	1	29.000	38.450	-9.450	-1.334	29.549	47.351	20.628	56.273
14	1	19.000	22.158	-3.158	-0.446	14.733	29.583	5.025	39.291
15	1	11.000	11.868	-0.868	-0.123	3.771	19.966	-5.567	29.303
16	1	14.000	19.762	-5.762	-0.813	10.055	29.469	1.524	38.001
17	1	36.000	34.994	1.006	0.142	25.596	44.391	16.918	53.069
18	1	22.000	22.039	-0.039	-0.006	13.883	30.195	4.577	39.501

For clarity, Table 20 was created to show the comparison between experimental and predicted values

Table 20. Experimental and Predicted values of the entire input and output parameters compared

EXPERIMENTAL						PREDICTED					
Angular distortion, $\alpha(^{\circ})$	Bead width (mm)	Bead penetration (mm)	Vol weld metal deposited per second	Volume of wire melted (mm ³ /s)	Melting efficiency (%)	Angular distortion (Predicted)	Bead width (Predicted)	Bead penetration (Predicted)	Vol weld metal deposited per second (Predicted)	Volume of wire melted (Predicted)	Melting efficiency (Predicted)
2.71	8.50	9.24	190.07	83.76	49	2.551	8.628	7.963	170.700	83.745	42.010
4.52	8.10	5.14	100.75	117.24	14	4.518	8.734	6.861	145.223	117.241	21.573
6.77	12.20	7.18	210.51	184.26	14	6.457	8.282	5.453	98.608	184.234	2.146
2.97	12.80	10.12	345.86	83.76	44	2.942	8.240	8.727	206.086	83.762	32.097
5.08	5.20	8.25	114.54	117.24	10	5.173	8.828	7.814	196.020	117.245	12.715
4.09	9.75	4.39	114.28	184.26	28	4.213	7.432	7.154	121.628	184.358	27.664
2.32	6.10	11.26	194.38	117.24	28	2.068	5.625	8.197	145.120	117.310	24.860
3.86	5.85	10.76	178.14	184.26	36	3.773	7.345	8.245	164.596	184.319	32.326
5.79	10.25	11.00	319.08	83.76	20	5.719	10.797	9.440	283.909	83.827	19.609
4.06	8.92	5.63	121.53	184.26	22	4.323	7.382	6.278	105.004	184.149	22.375
3.74	7.15	4.66	80.63	83.76	10	3.897	7.981	6.682	129.160	83.797	16.275
5.45	7.05	9.81	167.37	117.24	24	5.307	10.281	7.318	180.367	117.274	27.079
3.68	8.16	6.42	139.87	117.24	29	3.827	9.475	9.095	237.561	117.193	38.450
3.39	3.25	8.42	73.06	184.26	19	3.425	5.885	6.697	86.484	184.325	22.158
4.94	8.22	6.96	152.75	83.76	11	5.076	9.140	7.903	199.689	83.846	11.868
2.80	3.03	4.94	42.36	184.26	14	2.769	4.855	7.338	103.780	184.278	19.762
4.80	12.47	9.22	325.38	83.76	36	4.745	10.961	10.177	304.596	83.789	34.994

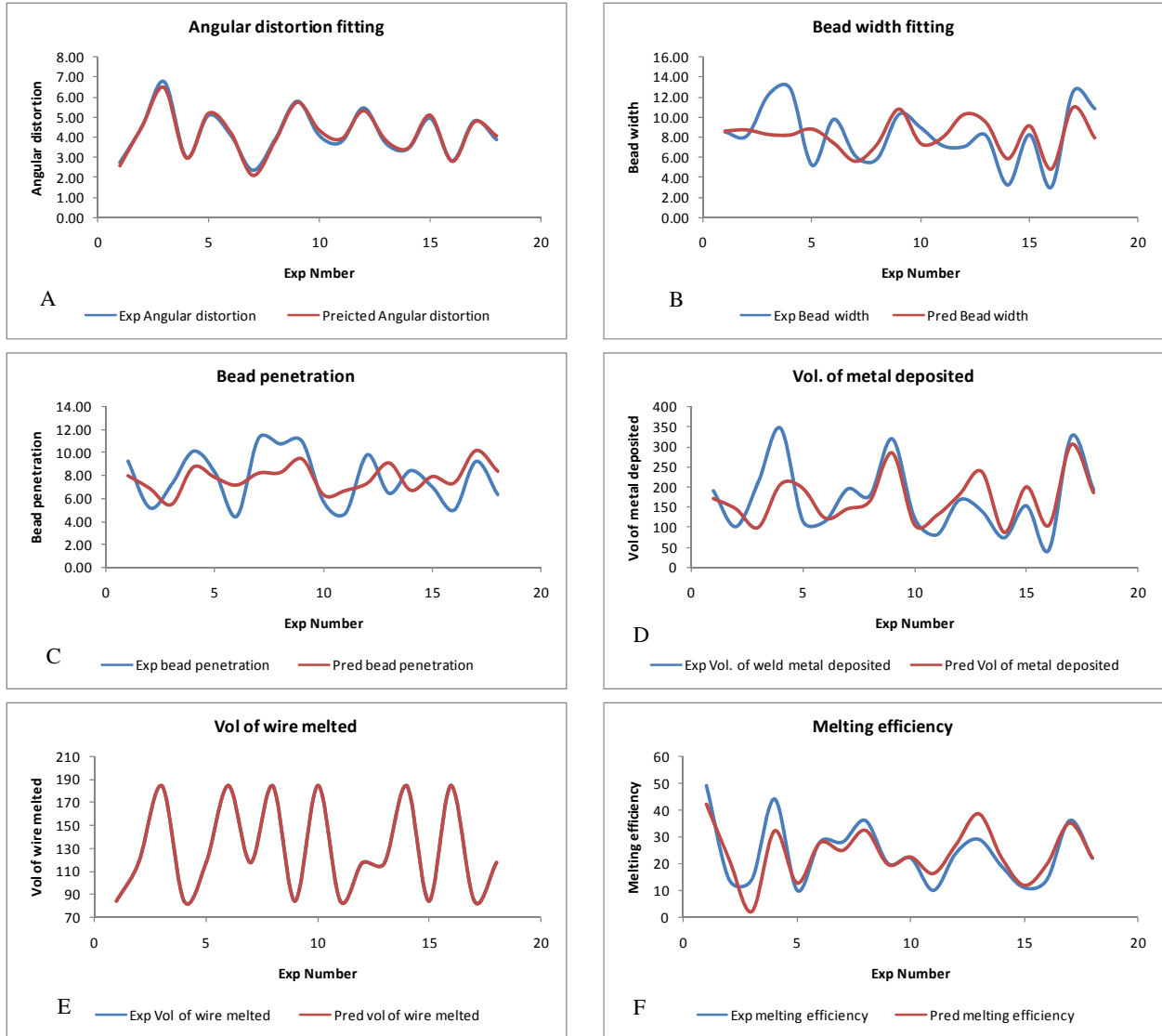


Fig. 1. Correlation between the predicted and calculated/measured output parameters

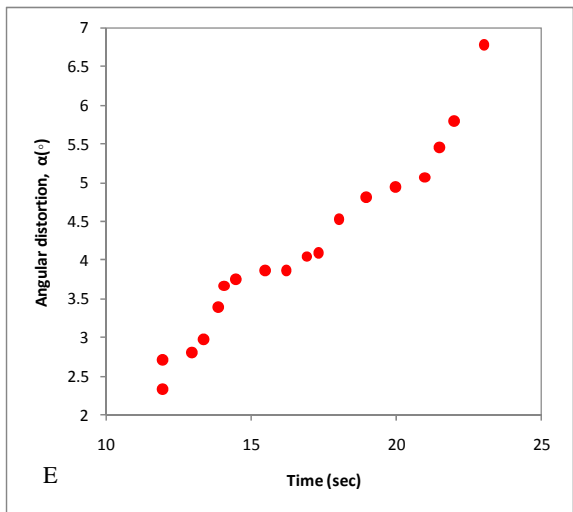
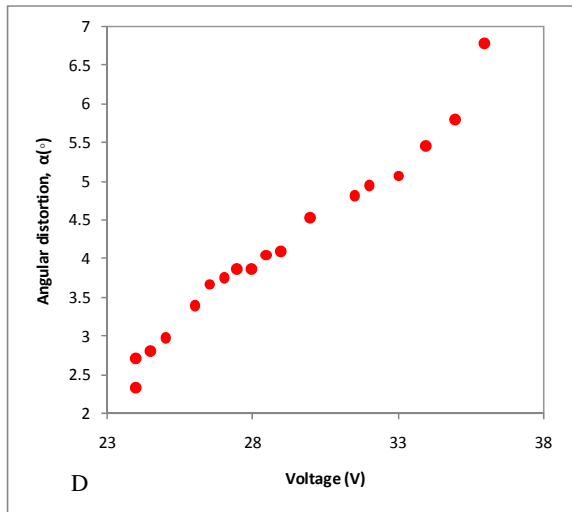
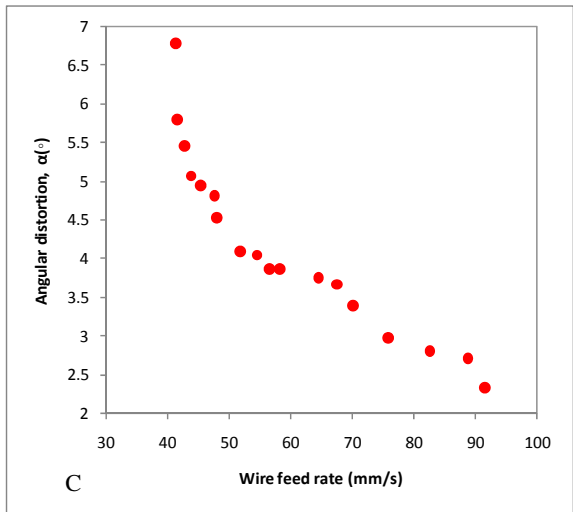
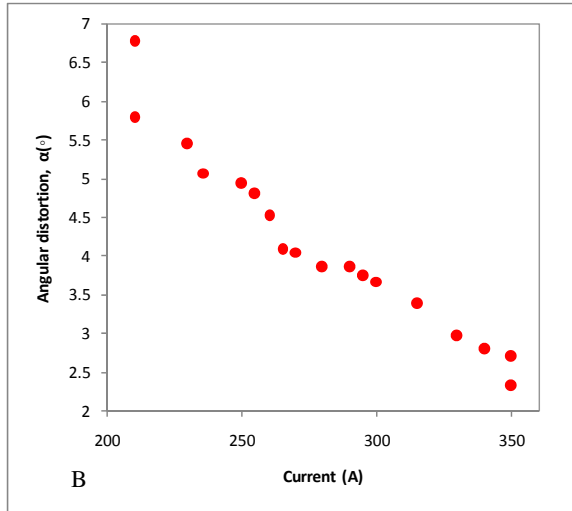
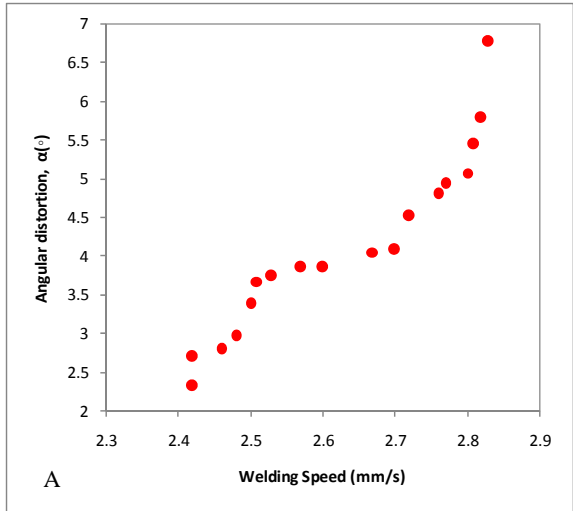


Fig. 2. Effect of Process Parameters on angular distortion

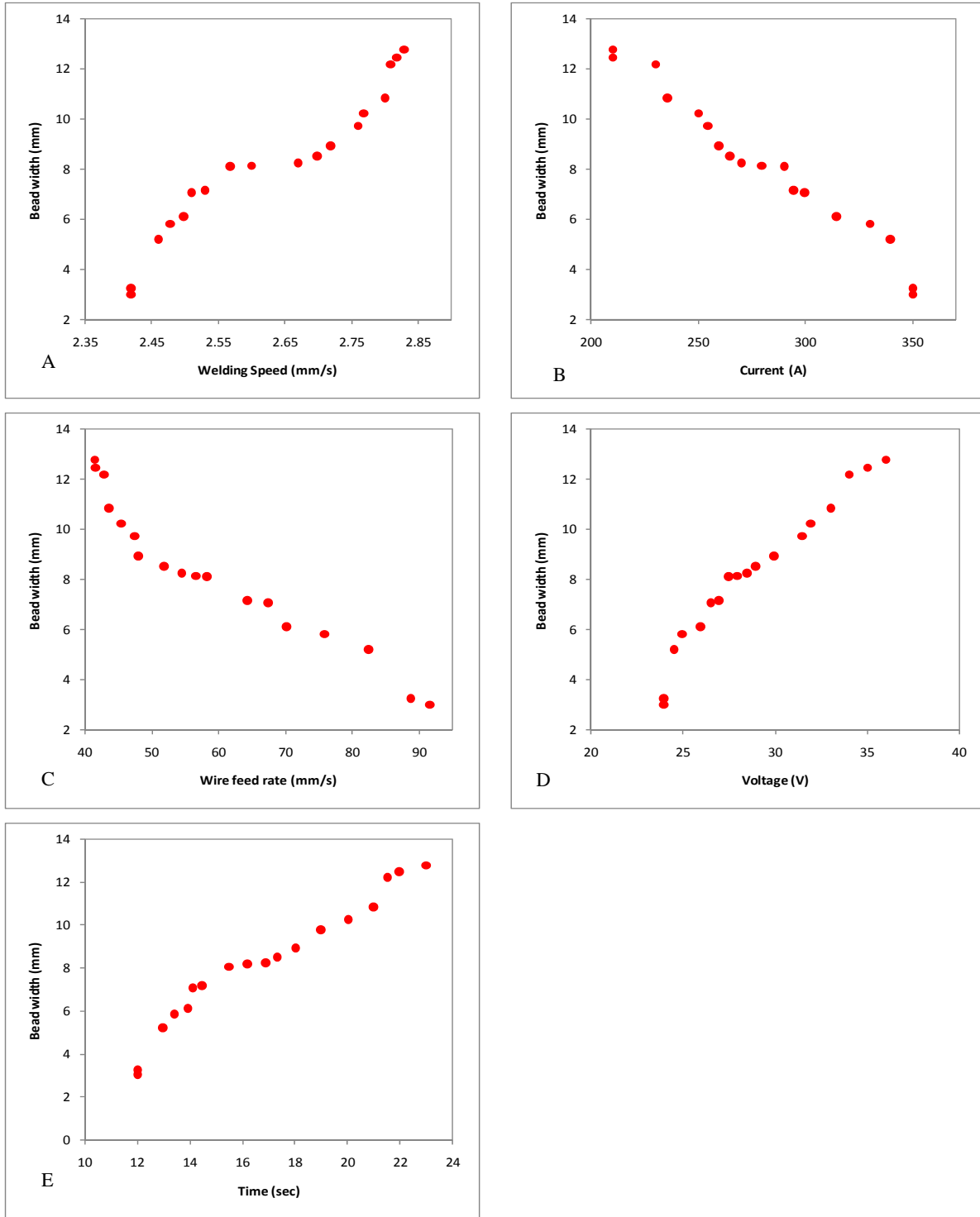


Fig. 3. Effect of Process Parameters on bead width

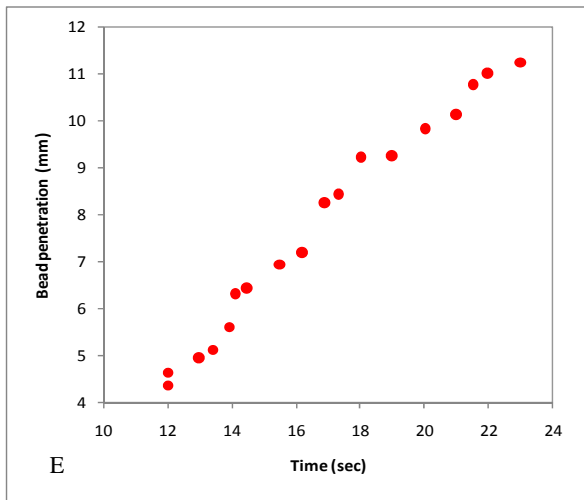
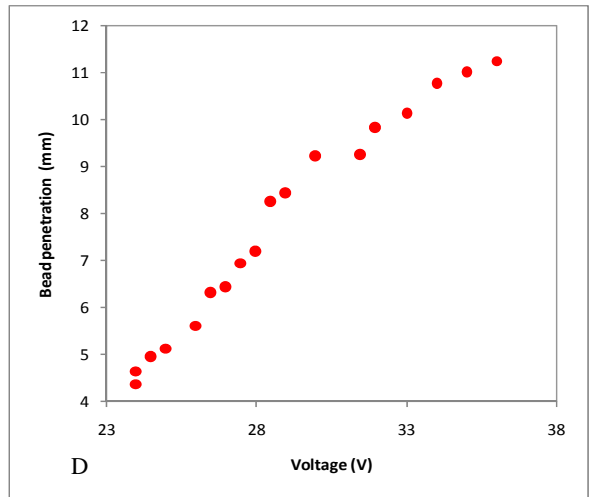
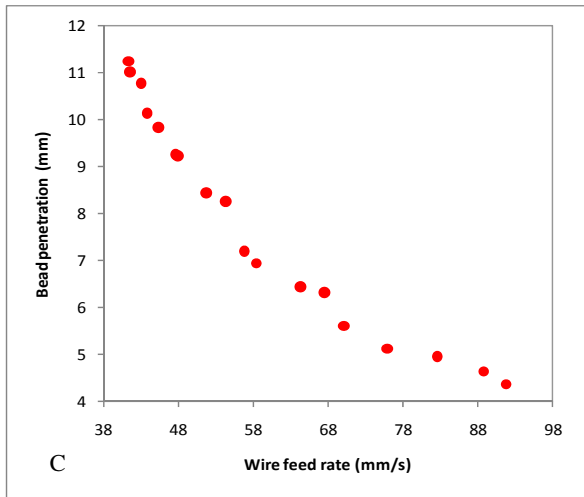
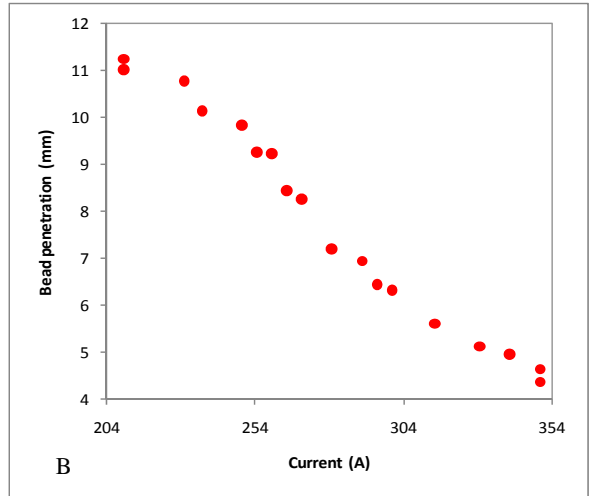
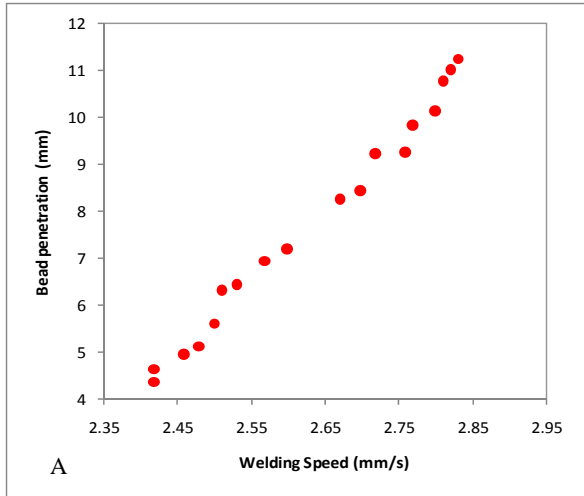


Fig. 4. Effect of Process Parameters on bead penetration

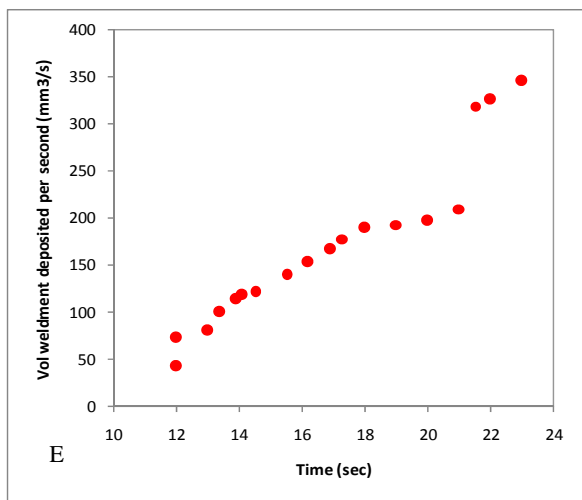
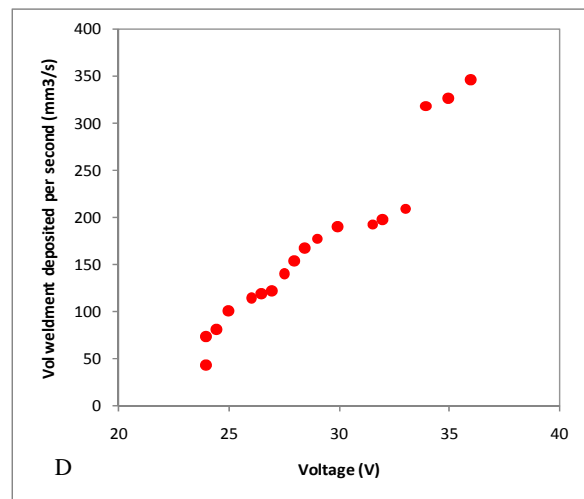
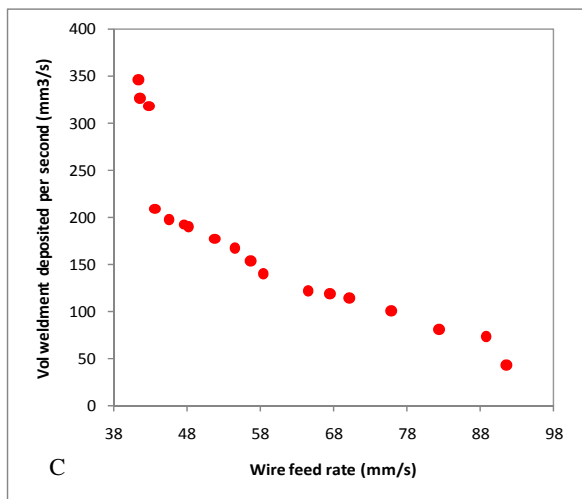
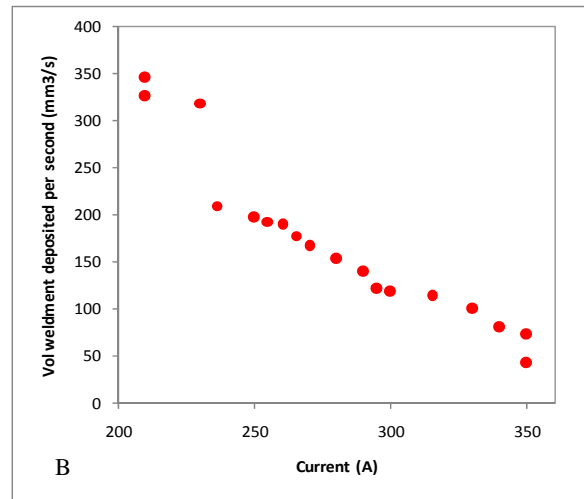
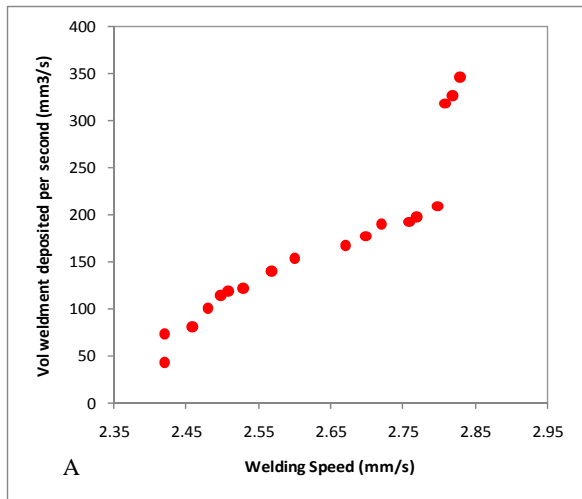


Fig. 5. Effect of Process Parameters on volume of weld metal deposited per second

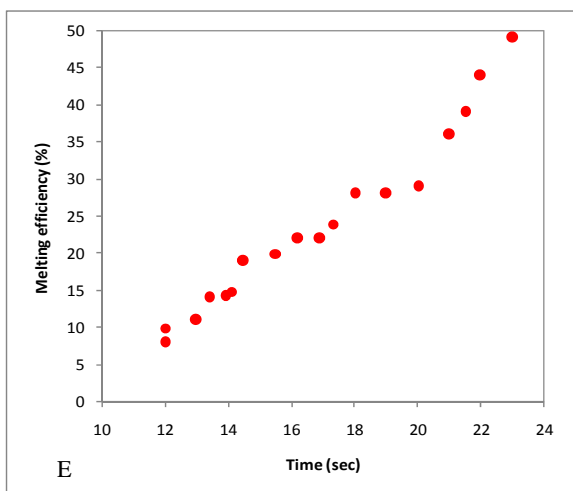
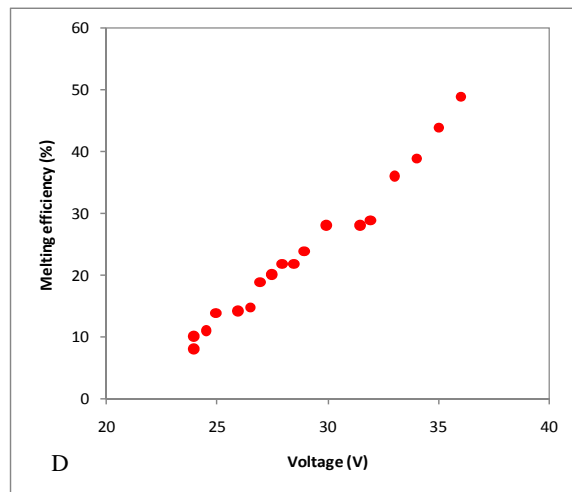
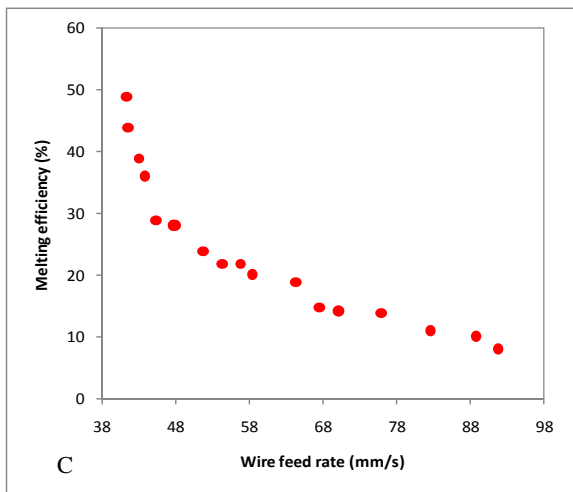
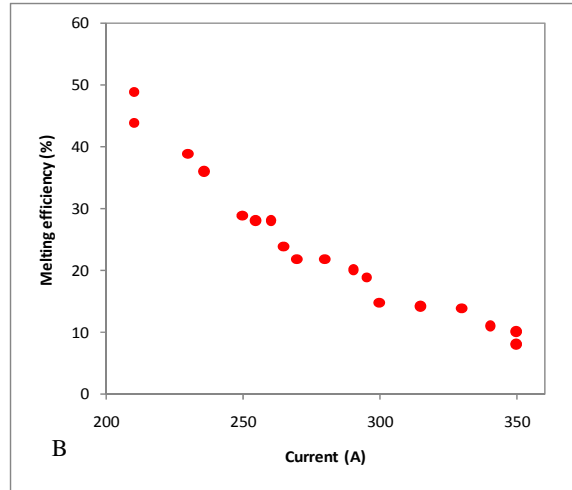
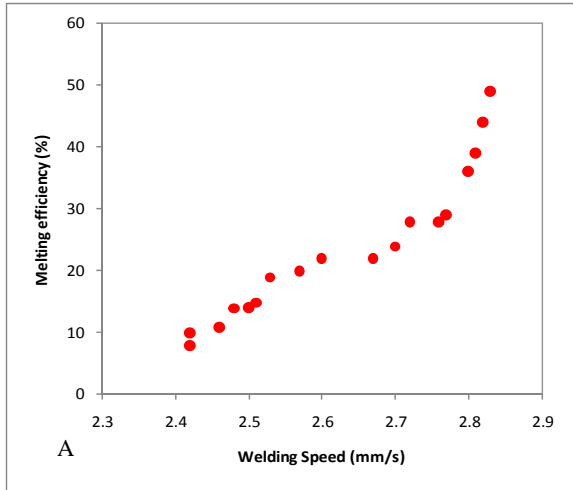


Fig. 6. Effect of Process Parameters on melting efficiency

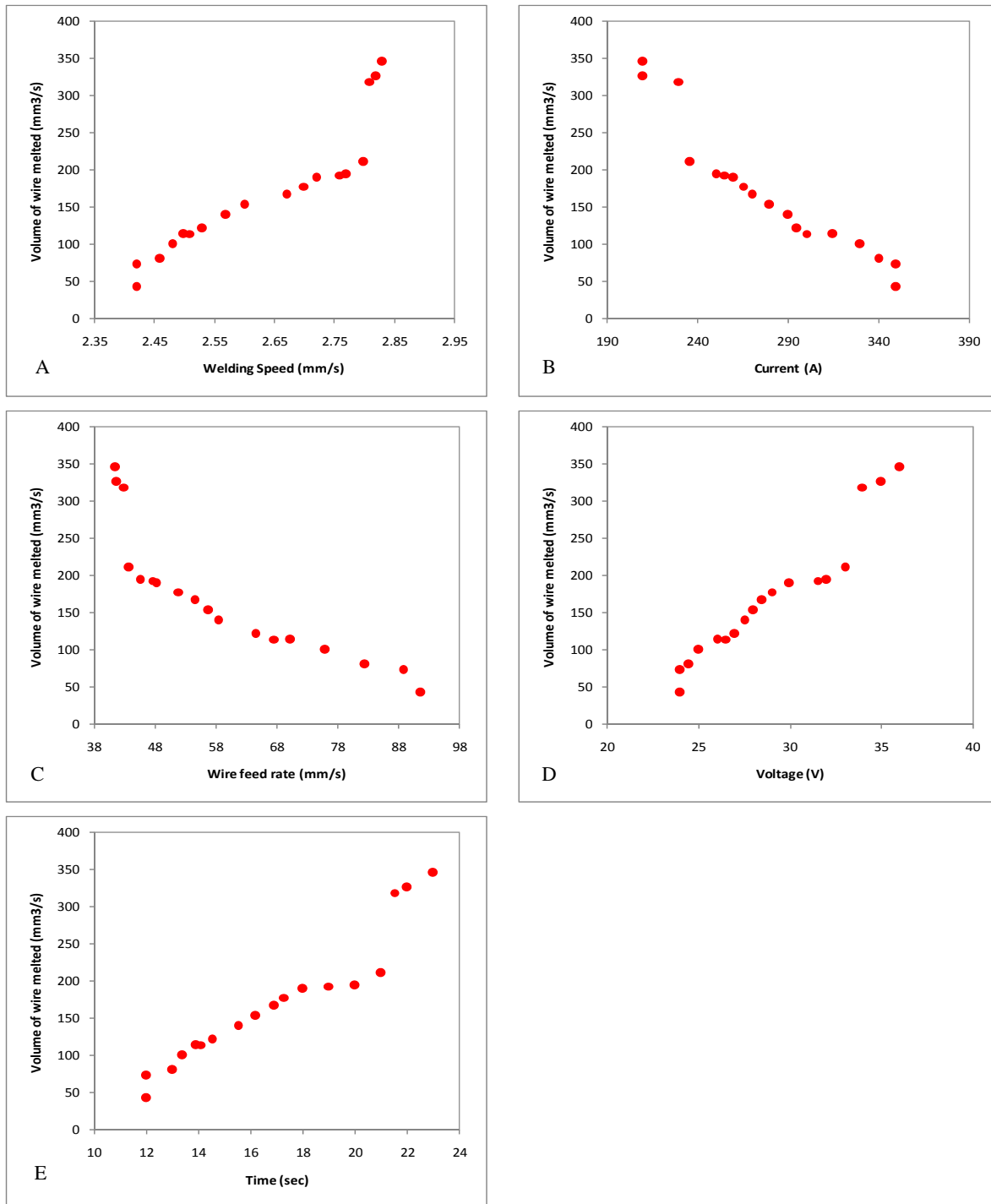


Fig. 7. Effect of Process Parameters on volume of wire melted

4.2 DISCUSSION

4.2.1 Correlation between Experimental and Predicted Values

Figure 1(a) shows the correlation between the experimentally calculated angular distortion and the predicted angular distortion using Eq. (6). From fig. 1(a), it can be seen that there is almost a perfect fit

between the calculated angular distortion and the predicted angular distortion. This indicates that the predicted model developed using regression analysis is very potent. Figure 1(b) shows the correlation between the experimentally measure bead width and the predicted bead width. From fig. 1(b), it can be seen that there are obvious variations in the correlation process. The predictive model shown in Eq. (7) could not accurately predict the bead width but the variations in their values are not too far apart.

Figure 1(c) shows the correlation between the experimentally measured bead penetration and the predicted bead penetration. From figure 1(c), it can be seen that the variations between the bead penetration measured values and predicted values are little bit far apart. The predictive model found in Eq. (8) has not been able to accurately predict the bead penetration but the predicted values are fairly close to the measured values. Figure 1(d) shows the correlation between the calculated volume of weldmetal deposited and the predicted volume of weldmetal deposited. It can be seen from figure 1(d) that the predictive model was able to predict the volume of weldmetal deposited with little variations when compared with the experimental calculated one. Figure 1(e) shows the correlation between the experimentally calculated volume of filler wire melted and its predicted values. From figure 1(e), it can be seen that there is a perfect match between the predicted and experimentally calculated volume of filler wire melted. The predictive model is very potent. Figure 1(f) shows the correlation between the predicted melting efficiency and the calculated melting efficiency. From fig. 1(f), it can be seen that there is a close correlation between the calculated melting efficiency and the predicted one. However, there is some little variation between their values. The predictive model is indicated in Eq. (11) is potent.

4.2.2 Effect of Process Parameters on Weld Metal Melting Profile

Figure 2(a) shows that the relationship between the angular distortion and the welding speed. Murugan and Gunaraji [9] were of the opinion that angular distortion is a major problem, most pronounced among different types of distortion in the butt welded plates. The authors said that angular distortion is mainly due to non-uniform transverse shrinkage along the depth of the plates welded. From figure 2(a), it is observed that between the angular distortion of 2.25° and 2.75° the welding speed of 2.4mm/s remains unchanged. As the welding speed increases from 2.4mm/s to 2.52mm/s, the angular distortion increases from 2.75° to 3.75° . At 3.75° , the residual stresses' generated by the continuous increase in the angular distortion have reached their peak and therefore begin to degenerate into a notch like structure. As the welding speed advances from 2.5mm/s to 2.8mm/s, the angular distortion gradually increases from 4° to 6.75° . The observations above show that there is a positive correlation between the welding speed and angular distortion.

Mandal and Parmar [10] used the two level full factorial techniques to develop mathematical models and reported that welding speed had a positive effect on angular distortion for single pass or multiphase welding. Figure 2(b) shows the relationship between welding current and angular distortion. From figure 2(b), it can be seen that as the welding current increases, the angular distortion reduces. This indicates that the increase in current refines the microstructure. This eventually produces a denser and more controllable weldment that is much less susceptible to distortion. However, when the current reduces to 210A, the angular distortion obtained can be very high an uncertain. The mild steel weldment is termed to be uncertain because two angular distortions of 5.75° and 6.75° occurred simultaneously and steeply too. The jump from 5.75° to 6.75° at a particular current shows the extent of strain that would have occurred in the weldment. This indicates that the grains in the weld microstructure are macro grains. Figure 2(c) shows that relationship between the wire feed rate and angular distortion of the material. From figure 2(c), it can be seen that as the wire feed rate increases, the angular distortion of the weldment material decreases. This indicates that as the wire feed rate increase, more bare electrodes are consumed. These consumed electrodes can also be a form of weldment reinforcement that can limit angular distortion of the weldment from expanding. When there is deep weld penetration achieved during welding, weld reinforcement could be firmer and more robust and angular distortion reduced to its bare-minimum. Wire feed rate of 40mm/s intends to be the major feed rate that can cause a massive occurrence of angular distortion of weldment. Figure 2(d) shows the relationship between voltage and angular distortion of the weldment. From figure 2(d), it is seen that as the voltage increases, the angular distortion also increases. This indicates that contrary to the effect of current on the angular distortion, the voltage exerts some pressure on the molten weld metal which strains the solidified weld metal and alters the weld microstructure. As the voltage is increased, the strain on the weld also increases. This increase in strain

would eventually adversely affect the weldment. Figure 2(e) shows the relationship between welding time and the weld angular distortion. From figure 2(e), it can be seen that as the welding time increases, the angular distortion also increases. This indicates that as the welding time increases, the heat treatment of the welded materials also increases. The increase in heat can lead to weld spatter, which eventually reduces the quality of the weld by increasing its angular distortion. Figure 3(a) shows the relationship between welding speed and bead width. From figure 3(a) it can be generally inferred that as the welding speed increases, the bead width also increases. This shows that as the welding time is reduced, the formation of the bead width is prolonged and the bead formed so far may be exposed to moisture which produces coarse and angular microstructure. These features reduce the quality of the weld. The welding speed of between 2.55mm/s and 2.70mm/s, appear not to affect the geometry of the weld bead width. This indicates that, at that range of welding speed, the weld bead with 9mm remain unaltered. Figure 3(b) shows that relationship between welding current and weld bead width. From figure 3(b), it can be seen that as the welding current increases, the bead width reduces. This shows that the welding current refines the weld microstructure into finer grains or molecules which increases the density of the weld and controls weld spatter. These features eventually improve the weld quality and as such, the bead width is controlled. Achebo and Odinikuku [11] were of the opinion that the smaller the bead width, the better the quality of the weldment. Therefore, in this case, the current is a vital process parameter responsible for the improvement of the quality of the weldment.

Figure 3(c) shows the relationship between wire feed rate and bead width. From figure 3(c), it can be seen that as the wire feed rate increases, the weld bead width reduces. This indicates that as the wire feed rate increases, the welding speed also increases as well as the welding time. These features effectively make a good quality weld with adequate penetration, thereby creating a weld bead with small bead width geometry. Figure 3(d) shows the relationship between the voltage and weld bead width. From figure 3(d), it can be seen that as the voltage increases, the weld bead width also increases. This indicates that the voltage has significant effect on the bead width. The voltage exerts some pressure on the bead geometry, as a result too many weld metal are deposited on the gap between the parent metals and these weld metals uncontrollably expand the dimensions of the bead geometry, thereby reducing the quality of the weldment. Figure 3(e) shows the relationship between the welding time and the bead width. From figure 3(e), it can be seen that as the welding time increases, the bead width is also increased. This shows that the prolonged heat treatment of the welding operation allows the deposition of lots of weld metal which makes it uncontrollably difficult to reduce the weld bead geometry such as the width. However, it can be observed that between the welding time of 15 seconds and 17 seconds, the bead width of 8.5mm is unaltered. This indicates that, as these welding times, the strain that occur at the weldmetal does not cause any further change in the bead width of 8.5mm/

Figure 4(a) shows that the relationship between the welding speed and weld bead penetration. From fig. 4(a), it can be seen that as the welding speed increases, the bead penetration also increases. This shows that as the welding time also reduces the molten weld metal flow experiences a Marangoni flow which flows into the gap of the parent metals that are being welded together, in a well guided manner and eventually achieving a deep penetration. Achieving a satisfactory depth of weld penetration reinforces the strength of the welded structure. Figure 4(b), it can be seen that as the current welding current and the bead penetration. From fig. 4(b), it can be seen that as the current increases, the bead penetration reduces. This indicates that, in this particular case, the current does not have significant effect on the bead penetration. The currents used in this study do not produce enough arc heat to melt sufficiently the filler metals that would fill the gap in between the parent metals to be welded together. Therefore, it can be concluded that current is not a major contributor to achieving an improved weld penetration geometry. Figure 4(c) shows that the relationship between wire feed rate and weld bead penetration. From fig. 4(c), it can be seen that as the wire feed rate increases, the bead penetration reduces. This indicates that increased wire feed rate over a very limited period of time would not have been able to produce enough molten weld metal to make adequate bead penetration. Figure 4(d) shows the relationship between voltage and bead penetration. From fig. 4(d), it can be seen that as the voltage increases, the bead penetration also increases. This shows that the voltage exert enough pressure that strains the molten filler metal, this causes easy detachment of molten metal from the electrode/filler metal tip and the gap of the parent metals that are to be welded together and this process eventually causes large deposition of molten weldmetal, thereby achieving a deep penetration of the weld metal. Figure 4(e) shows the

relationship between the welding time and weld bead penetration. From fig. 4(e), it can be seen that as the welding time increases, the bead penetration also increases. This shows that prolonged welding time allows for a lot of molten weld metal deposition which influences deep weld metal penetration.

Figure 5(a) shows the relationship between the welding speed and the volume of deposited weldmetal. From fig. 5(a), it can be seen that as the welding speed increases, the volume of weldmetal deposited also increases. This melting process results in increase deposition of molten weldmetal which eventually increases the volume of the deposited weldmetal. Figure 5(b) shows the relationship between the welding current and the volume of deposited weldmetal. From fig. 5(b), it can be seen that as the current increases, the volume of the deposited weldmetal decreases. This indicates that as the arc heat increases, the filler metal melts and forms spatter. The spatter reduces the volume of weldmetal deposited into the gap of the parent metal to be welded. Figure 5(c) shows the relationship between wire feed rate and the volume of deposited weldmetal. From fig. 5(c), it can be seen that as the wire feed rate increases, the volume of weldmetal deposited reduces. This can be attributed to the fact that when the wire feed rate increases, the amount of filler wire used is reduce therefore the volume of weld metal deposited is expected to be reduce. However, wire feed rate of 42.5mm/s appears to have incompletely high deposition of molten weldmetal and can be seen as uncertain because there is a noticeable gap in the volume of weldmetal deposition, which is between 120mm³/s and 320mm³/s. Figure 5(d) shows the relationship between the wire feed rate and volume of weldmetal deposited. From fig. 5(d), it can be seen that as the voltage is increasing, the volume of deposited weldmetal is also increasing. This indicates that the pressure exerted by the voltage causes a strain on the molten filler wire, which facilitates the detachment of molten metal droplets from the filler wire, this process eventually increases the volume of deposited weldmetal into the gap between the parent metals to be welded together. However, voltage of 33V appears not to be certain in the sense of the fact that there was discontinuity in the deposition of molten weldmetal. Figure 5(e) shows the relationship between the welding time and the volume of the deposited weldmetal. From fig. 5(e), it can be seen that as the welding time increases, the volume of the deposited weldmetal also increases. This indicates that, because there was prolong heat treatment on the filler wire, the amount of filler wire melted was so many and this eventually increased the volume of weldmetal deposited. However, as the welding time of 21 seconds, there is a discontinuity in the deposition of molten weldmetal. This could be as a result of influx of interfering atmospheric air in to the welding environment. This could cause the oxidization of the molten weldmetal, making the molecules enlarges, causing disruption in the flow of molten weldmetal which eventually causes a discontinuity in the deposition of molten weldmetal.

Figure 6(a) shows the relationship between the welding speed and the melting efficiency of the welding process. From fig. 6(a), it can be seen that as the welding speed increases, the melting efficiency of the welding process also increases. This indicates that the welding speed facilitates the detachment of the electrode wire droplets by localizing the arc heat on the electrode wire. This process eventually sufficiently, in a guided manner, effectively melts the electrode wire in order to achieve deep weld penetration. However, a welding speed of 2.78mm/s and 2.9mm/s produces melting efficiencies of between 27% and 50% as recorded in literature by other researchers. Figure 6(b) shows the relationship between the welding current and melting efficiency. From fig. 6(b), it can be seen that as the welding current increases, the melting efficiency reduces. This indicates that either the current may not have produced sufficient heat to melt the electrode wire or the current may have produce intense arc heat that would have cause weld spatter and highly heterogeneous filler wire melting phenomena which would eventually affected the melting pattern of the entire welding process. Figure 6(c) shows the relationship between the wire feed rate and the melting efficiency of the welding process. From fig. 6(c), it can be seen that as the wire feed rate increases, the melting efficiency reduces. This indicates that as the wire feed rate increases, it lowers the welding time and this does not allow sufficient heat on the localized welding point between the electrode tip and the workpiece thereby causing melting of the electrode wire into the gap between the parent metal that are to be welded together the parent metal that are to be welded together. This process lowers the melting efficiency of the entire welding operation. Figure 6(d) shows the relationship between the welding voltage and the melting efficiency. From fig. 6(d), it can be seen that as the voltage increases, the melting efficiency of the filler wire also increases. This indicates that the voltage that the voltage exert enough pressure to cause the required filler wire droplets that would cause controlled melting pattern which is expected to achieve deep weld penetration in between

the gap created by the parent metals to be welded together. Voltages of 28.5V and 31V appear to be unaltered in making the melting efficiency of 28%. Figure 6(e) shows the relationship between welding time and melting efficiency. From fig. 6(e), it can be seen that as the welding time increases, the melting efficiency also increases. This indicates that as the welding process is prolonged, more filler wires are melted and deep weld penetration is achieved. As a result of the melting efficiency in the filler wire melting process, the melting efficiency eventually optimized. However, welding time of 18 seconds and 23 seconds produced the welding operation that has melting efficiencies of between 27.5% and 50%. Figure 7(a) shows the relationship between welding speed and volume of wire melted. From fig. 7(a), it can be seen that as the welding speed increases, the volume of filler wire melted also increases. This indicates that as the speed of the welding process increases, more filler wires are melted and the volume of deposited molten filler wire increases. This increase in the filler wire deposition helps to achieve deep weld penetration. From literature, it was researched that filler wire deposits over 95% of the volume of the entire molten weldmetal deposited in the gap between the parent metals to be welded. About 5% of the deposited volume of weldmetal comes from the heat affected zones of the melted parent metals. Figure 7(b) shows the relationship between the welding current and the volume of wire melted. From fig. 7(b), it can be seen that as the welding current increases, the volume of the filler wire melted reduces. This indicates that the voltage does not exert enough pressure to detach the weldmetal droplets from the filler wire tip as compared to the required number of welding cycles needed to sufficiently produce a satisfactory volume of molten weldmetal. Figure 7(c) shows the relationship between the wire feed rate and volume of wire melted. From fig. 7(c), it can be seen that as the wire feed rate increases, the volume of wire melted reduces. This indicates that as the wire feed rate increases, the time spent on heating and melting the filler wire is reduced. This process eventually reduces the volume of filler wire weldmetal produced. Figure 7(d) shows the relationship between the voltage and the volume of wire melted. From fig. 7(d), it can be seen that as the voltage increases, the volume of the filler wire melted also increases. This indicates that the voltage exerts enough pressure required to detach the molten weld metal droplets from the heated filler wire tips. These droplets formed under constrained heated environment, build up into large volume of melted filler wires. Figure 7(e) shows the relationship between welding time and volume of filler wire melted. From fig. 7(e), it can be seen that as the welding time increases, the volume of filler wire melted also increases. This indicates that as the welding time is prolonged, the number of filler wire melted increases and this process eventually increased the volume of filler wire that would be melted. When a large volume of melted filler wire is achieved, a deep weld penetration would also be achieved.

4. CONCLUSION

Mild steel filler wire and parent metal heat affected zone melting profiles have been studied. This study includes the determination of the angular distortion of welded plates weld bead geometry, volume of deposited weldmetal which came from the heat affected zones of the parent material and the filler wire, the volume of melted filler wire that is said from literature to constitute about 95% of the entire volume of the deposited weldmetal and the volume of the deposited weldmetal and the melting efficiency of the entire welding process was also investigated in this study. The range of the melting efficiency fell within the range of the ones reported in literatures. However, the effects of the input process parameters on the output parameters that makeup the melting profile were also investigated. These output parameters which are the angular distortion, bead width, bead penetration, volume of weldmetal deposited, volume of filler wire melted and melting efficiency were all predicted using the regression analysis. A correlation analysis was also done to determine the adequacy and the potency of the model and it was discovered that some predictive models were able to predict the output parameters accurately while others have little variations between the experimentally measured and the predicted values. In this study, the melting profile of mild steel weldment has been successfully investigated and the volume of deposited weldmetal has also been successfully determined in this study.

ACKNOWLEDGEMENT

The authors wish to acknowledge the efforts of Prof. Joseph Achebo for the success of this work.

COMPETING INTERESTS

Authors have declared that no competing interests exist.

REFERENCE

1. Lee, J I. and Um K. W. (2000), A Prediction of Welding Process Parameters by prediction of back bead geometry, *Journal of Materials Processing Technology*, Vol. 108, Issue I, pp. 106-113 Doi: 10.1016/S0924- 0136(00)00736-6
2. Gunaraj V. and Murugan, N. (2000), Prediction and Optimization of Weld Bead Volume for the Submerged Arc Process-Part1. *Welding Journal* pp. 2865-2945.
3. Sreeraj, P.; Kannan, T. and Maji, S. (2013) Prediction and Optimization of Weld Bead Geometry in Gas Metal Arc Welding Process using RSM and Fminco. *Journal of Mechanical Engineering Research*. Vol. 5, (8), pp. 154 – 165. Doi: 10.5897/JMER2013.0292.
4. Lalitnarayan, K.; Sarcar, M.M.M.; MallikarjunRoa K. and Kameswaran, K. (2011). Prediction of Weld Bead Geometry for CO₂ Welding Process by Multiple Regression Analysis. *International Journal of Mathematics and Scientific Computing*, Vol. 1, No 1, pp. 52 – 57.
5. Karthikeyan R. and Balasubramanian V. (2010). Prediction of the Optimized Friction Stir Sport Welding Process Parameters for Joining AA2024 Aluminum Alloy using RSM. *The International Journal of Advanced Manufacturing Technology*. vol. 51, Issue 1-4, pp. 173 – 183. Doi: 10.1007/s00170-010-2618-2.
6. Pilipenko, A. (2001). Computer Simulation of Residual Stress and Distortion of Thick Plates in Multi-Electrode submerged Arc Welding – their Mitigation Techniques. Ph.D. Thesis. Norwegian University of Science and Technology, Norway.
7. Ivanov, N.A. and Ulanov, A.M. (). The Methodology of Calculation of the Geometric Sizes of the Welds on the Parameters of the Model of Automatic Arc Welding under a layer of flux (www.97-ivanov_ENG.pdf)
8. Dupont, J.N. & Marder, A. R. (1995). Thermal efficiency of arc welding processes. 74. 406-s.
9. Murugan, V.V. and Gunaraji, V. (2005). Effects of Process Parameters on Angular Distortion of Gas Metal Arc Welded Structural Steel Plates. *Welding Journal*, pp: 165s -171s.
10. Mandal, A. and Parmar, R.S. (1997). Effect of Process Variables and Angular Distortion of Pulse GMAW welded HSLA plates. *Indian Welding Journal*, pp. 26 – 34.
11. Achebo, J. and Odinikuku, W. E. (2015) Optimization of Gas Metal Arc Welding Process Parameters Using Standard Deviation (SDV) and Multi-Objective Optimization on the Basis of Ratio Analysis (MOORA). *Journal of Minerals and Materials Characterization and Engineering (JMMCE)*, 3, 298 - 308